Allele-Specific Editing of a Dominant *SCN8A* Epilepsy Variant Protects against Seizures and Lethality in a Murine Model

Wenxi Yu, PhD,[1] Sophie F. Hill, PhD,[1,2] Yumei Huang, PhD,[3] Limei Zhu, PhD,[4] Yiannos Demetriou, BS,[4] Julie Ziobro, MD, PhD,[5] Faith Reger, MS,[1] Xiaoyan Jia, PhD,[3] Joanna Mattis, MD, PhD,[4] and Miriam H. Meisler, PhD[1,2]

Objective: Developmental and epileptic encephalopathies (DEEs) can result from dominant, gain of function variants of neuronal ion channels. More than 450 de novo missense variants of the sodium channel gene *SCN8A* have been identified in individuals with DEE.
Methods: We studied a mouse model carrying the patient *Scn8a* variant p.Asn1768Asp. An AAV-PHP.eB virus carrying an allele-specific single guide RNA (sgRNA) was administered by intracerebroventricular injection. Cas9 was provided by an inherited transgene.
Results: Allele-specific disruption of the reading frame of the pathogenic transcript generated out-of-frame indels in 1/4 to 1/3 of transcripts throughout the brain. This editing efficiency was sufficient to rescue lethality and seizures. Neuronal hyperexcitability was reduced in cells expressing the virus.
Interpretation: The data demonstrate efficient allele-specific editing of a dominant missense variant and support the feasibility of allele-specific therapy for DEE epilepsy.

ANN NEUROL 2024;96:958–969

Epileptic disorders have an incidence of >1% in the United States (US) population.[1] Variants in more than 100 genes have been associated with these disorders. One third of the identified genes encode neuronal ion channels, including the voltage-gated sodium channel genes *SCN1A*, *SCN2A*, and *SCN8A*.[2] Developmental and epileptic encephalopathy (DEE) is a severe form of epilepsy characterized by refractory seizures, sudden unexpected death in epilepsy (SUDEP), motor and gastric dysfunction, and intellectual disability.[3–5] More than 450 variants in *SCN8A* have been reported in patients with DEE.[6,7]

SCN8A encodes the voltage-gated sodium channel $Na_v1.6$, which is highly enriched in the distal axon initial segment and at nodes of Ranvier and functions in initiation and propagation of action potentials.[8] Many pathogenic variants of *SCN8A* result in gain-of-function (GOF) effects on channel activity, including premature channel opening and impaired channel inactivation.[3,9–11] Expression of *Scn8a* GOF variants either in excitatory[12,13] or inhibitory neurons[14,15] can both cause seizures.

Fifty percent reduction of *Scn8a* expression by intracerebroventricular (ICV) administration of *Scn8a*-antisense oligonucleotides (ASOs) reduces seizures and extends

View this article online at wileyonlinelibrary.com. DOI: 10.1002/ana.27053

Received Apr 11, 2024, and in revised form Jun 18, 2024. Accepted for publication Jul 26, 2024.

Address correspondence to Dr Meisler, Department of Human Genetics, University of Michigan Medical School, 4909 Buhl Box 5618, Ann Arbor, MI 48109-5618. E-mail: meislerm@umich.edu

From the [1]Department of Human Genetics, University of Michigan, Ann Arbor, MI; [2]Neuroscience Graduate Program, University of Michigan, Ann Arbor, MI; [3]Center for Genomic Technologies, Greater Bay Area Institute of Precision Medicine (Guangzhou), Fudan University, Guangzhou, China; [4]Department of Neurology, University of Michigan, Ann Arbor, MI; and [5]Department of Pediatrics, University of Michigan, Ann Arbor, MI

Additional supporting information can be found in the online version of this article.

 © 2024 The Author(s). *Annals of Neurology* published by Wiley Periodicals LLC on behalf of American Neurological Association.
This is an open access article under the terms of the Creative Commons Attribution-NonCommercial-NoDerivs License, which permits use and distribution in any medium, provided the original work is properly cited, the use is non-commercial and no modifications or adaptations are made.

survival.[16,17] Repeated *Scn8a*-ASO administration after seizure onset provided long-term protection to *Scn8a*-DEE mice.[18] However, limitations of ASO treatment include the need for repeated administrations and the difficulty in controlling the effect on gene expression. Reduction of *SCN8A* expression below 50% could exacerbate the deleterious effects seen in haploinsufficiency, which include intellectual disability,[19,20] seizures,[6,21] ataxia,[22,23] and dystonia.[24]

Advances in genome editing now permit allele-specific inactivation of a dominant pathogenic allele in heterozygotes. This strategy requires only a single treatment and protects the normal allele, preserving a minimum of 50% of wild-type (WT) *SCN8A* expression in cells and reducing potential adverse effects from excessive downregulation of the target gene. Successful examples of allele-specific targeting include improved hearing in mouse models of dominant deafness by delivery of single guide RNA (sgRNA)/Cas9 to the inner ear.[25–27] Allele-specific editing of the retinitis pigmentosa variant RHO^{T17M} by administration of sgRNA/Cas9 to the eye also resulted in a long-term improvement of retinal function.[28]

To evaluate allele-specific editing for treatment of epilepsy, we used a mouse model carrying the dominant patient variant *Scn8a*-N1768D. This mouse line was generated by transcription activator-like effector nucleases (TALEN) targeting, with introduction of the pathogenic A > G substitution as well as 8 nearby silent base substitutions that prevent correction of the pathogenic change.[29] This cluster of single nucleotide polymorphisms (SNPs) allowed us to design sgRNAs with 3 or 4 differences from the WT allele. (The missense variants in human *SCN8A*-DEE result from single nucleotide substitutions, only some of which can be targeted with current CRISPR/Cas9 technology.) The untreated $Scn8a^{N1768D/+}$ mice exhibit seizure onset between 2 and 3 months of age, and lethality by 5 to 6 months.[16,18,30] Here, we demonstrate rescue of the disorder by allele-specific inactivation of the pathogenic allele. This result extends the feasibility of genome editing to treatment of epilepsy and other dominant neurological disorders.

Methods

Mice

$Scn8a^{N1768D/+}$ (D/+) mice (JAX stock 039107) were generated in our laboratory and maintained by backcrossing to strain C57BL/6J (JAX stock 000664) for more than 30 generations.[29,30] Mice were housed and cared for in accordance with National Institutes of Health (NIH) guidelines in a 12/12 hour light/dark cycle with standard mouse chow and water available ad libitum. Animal experiments were approved by the Institutional Animal Care and Use Committee at the University of Michigan in accordance with the National Institute of Health Guide for the Care and Use of Animals (protocol PRO00009797). Principles outlined in the ARRIVE guidelines and the Basel declaration (https://www.basel-declaration.org/) including the 3R concept have been considered when planning experiments. Cas9/Cas9 homozygous mice were purchased from the Jackson Laboratory (JAX stock 026179). D/+ mice were crossed with Cas9/Cas9 mice to generate D/+, Cas9/+ affected mice and Cas9/+ controls. Both male and female mice were used for experiments.

In vitro DNA Digestion by Cas9

Allele-specific DNA oligonucleotides were purchased from IDT. sgRNAs were synthesized using the EnGen sgRNA Synthesis Kit, *Streptococcus pyogenes* (NEB 3322, Ipswich, MA) and purified with the Monarch RNA Cleanup Kit (NEB T2050). SpCas9 nuclease was purchased at 1μM concentration (NEB M0386S). One kb DNA fragments containing the sgRNA targeted sequence were amplified by polymerase chain reaction (PCR) from genomic DNA of WT or $Scn8a^{N1768D/N1768D}$ mice using primers F: 5′-CCC TGC TCT TTG CCT TAA T-3′ and R: 5′-TTT GCC TCT TGG CTC TTT C-3′. Amplified DNA was purified with the QIAquick PCR Purification Kit (Qiagen 28106, Germantown, MD). In vitro DNA digestion was performed according to manufacturer's instructions (NEB M0386). In brief, 27μl reactions were constituted with 1× NEBuffer r3.1, 30nM sgRNA, and 30nM SpCas9 nuclease and incubated at 25°C for 10 minutes to permit assembly of the Cas9/sgRNA ribonucleoprotein (RNP) complex. A total of 3μl of WT or $Scn8a^{N1768D}$ DNA fragments (30nM) were added and the reactions were incubated at 37°C for 15 minutes. One unit of Protease K was added to terminate the reaction and incubated at room temperature for 10 minutes. Reaction products were analyzed by 1.5% agarose gels.

Allele-Specific Editing in Mouse Embryonic Fibroblasts

Allele-specific sgRNA-2 and sgRNA-3 were cloned into pSpCas9(BB)-2A-Puro (PX459) V2.0 plasmid (Addgene 62988, Watertown, MA). Plasmid DNA was purified with the ZymoPURE Plasmid Miniprep Kit (Zymo D4200, Irvine, CA). Mouse embryonic fibroblasts (MEFs) were isolated from $Scn8a^{N1768D/+}$ heterozygous embryos at E13.5 and grown in Dulbecco's Modified Eagle Medium containing 10% fetal bovine serum and 1× antibiotic antimycotic solution. After 2 passages, MEFs were transfected with sgRNA-expressing plasmids using Lipofectamine LTX (ThermoFisher 15338100) and selected with 2μg/ml puromycin starting at 48 hours post transfection for 6 days. Genomic DNA was extracted and sequenced by Amplicon-EZ sequencing (Azenta, Illumina, Burlington, MA). A 482 bp

DNA amplicon harboring the sgRNA targeted sequence with flanking adaptor sequence was amplified using the primer set F: 5′-ACA CTC TTT CCC TAC ACG ACG CTC TTC CGA TCT CCC TGC TCT TTG CCT TAA T-3′ and R: 5′-GAC TGG AGT TCA GAC GTG TGC TCT TCC GAT CTG GCA TCA GGA TCA AAC TTC T-3′.

Analysis of Amplicon-EZ Sequencing Data

The adapter sequence was first trimmed from paired-end Amplicon-EZ sequencing data. The adapter-trimmed reads returned by Azenta were mapped to the 482 bp WT allele sequence using BWA-MEM.[31] Only read 2 files were used for analysis because the sgRNA-targeted region is located in the middle of read 2. The mapped reads were extracted from bam files using SAMtools[32] (version 1.6) followed by classification into WT-allele reads, mutant-allele reads and unclassified. To this end, the BBDuk software of BBTools (version 38.18, written by Bushnell B.; https://sourceforge.net/projects/bbmap/) was used to distinguish WT from mutant allele based on unique sequence tags (sgRNA2-targeted samples, WT-specific tag "CATCTCC," mutant-specific tag "TATCTCT"; sgRNA3-targeted samples, WT-specific tag "CTTGGAGA," mutant-specific tag "TTTGGAGG"). Editing outcome figures were generated using CRISPResso2[33] (version 2.2.7). Custom R scripts were further used to quantify the total indel rate and out-of-frame indel rate using output files of CRISPResso2. Out-of-frame indel rate in this study was defined as the fraction of reads whose indel size was not divisible by 3.

Allele-Specific Editing in Mouse Brain

AAV-PHP.eB virus expressing the *Scn8a*^{N1768D} allele-specific sgRNA-2 paired with a BH-scaffold[34] and an eGFP fluorescent marker was prepared by the University of Michigan Vector Core. Virus (2µl, 1×10^{13}vg/ml) was administered to mice by ICV injection at postnatal day 1 (P1). Controls received ICV administration of 2µl phosphate-buffered saline (PBS) at P1. Brain was dissected into 6 regions (cortex, hippocampus, cerebellum, brain stem, spinal cord, and remaining tissue). Total RNA was prepared by TRIzol extraction using a Direct-zol RNA Miniprep Plus Kits (Zymo R2072). Complementary DNA (cDNA) was synthesized with the LunaScript RT SuperMix Kit (NEB E3010L) and indels were detected by Amplicon-EZ sequencing as previously described.

Acute Slice Preparation and Whole Cell Patch Clamp Electrophysrhebiology

An AAV-PHP.eB virus with the eGFP cassette replaced by the red fluorescent mKATE cassette was prepared by the University of Michigan Vector Core. Virus (2µl, 2.5×10^{13}vg/ml) was administered to D/+, Cas9/+ mice by ICV injection at P1. At 2 to 3 months post injection, mice were deeply anesthetized (via isoflurane) and brains were removed and transferred to ice-cold sucrose solution that contained, in mM: NaCl, 87; sucrose, 75; KCl, 2.5; $CaCl_2$, 1.0; $MgSO_4$, 2.0; $NaHCO_3$, 26; NaH_2PO_4, 1.25; glucose, 10) bubbled with 95% O_2 and 5% CO_2. Coronal brain slices (300µm thickness) were prepared using a Leica VT-1200S vibratome (Leica Microsystems, Buffalo Grove, IL). Slices were transferred to a recording chamber containing oxygenated artificial cerebrospinal fluid (ACSF) that contained, in mM: NaCl, 125; KCl, 2.5; $CaCl_2$, 2.0; $MgSO_4$, 1.0; $NaHCO_3$, 26; NaH_2PO_4, 1.25; glucose, 10). Slices recovered at 32°C for 30 minutes and at room temperature for 30 minutes before recording. During recording, slices were perfused with oxygenated ACSF in a bath maintained at 31°C. Dentate gyrus granule cells were imaged using the SliceScope microscope (Scientifica) and were identified based on location within the granule cell layer. Whole cell patch clamp recordings were performed using a SliceScope Pro 6,000 electrophysiology system (Scientifica, Clarksburg, NJ). Whole cell recordings were obtained from mKATE positive and mKATE negative cells using borosilicate glass electrodes, pulled using a P-97 puller (Sutter Instruments, Novato, CA) for a tip resistance of 3 to 4MΩ. Electrodes were filled with a K-gluconate internal solution that contained, in mM: K-gluconate, 130; KCl, 6.3; EGTA, 0.5; $MgCl_2$, 1.0; HEPES, 10; Mg-ATP, 4.0; Na-GTP, 0.3. The pH of the internal solution was adjusted to 7.30 with KOH and the osmolarity was adjusted to 285mOsm with 30% sucrose. Electrodes were positioned via a PatchStar manipulator (Scientifica). Data were only included for final analysis if the cell had a resting potential below −70mV. Series resistance compensation (bridge balance) was applied throughout current clamp experiments with readjustments as necessary. No liquid junction potential correction was performed.

Analysis of Whole-Cell Electrophysiology Data

Analysis was performed blind to genotype using custom Python software and the pyABF package (https://pypi.org/project/pyabf). Action potentials (APs) were defined as passing 0mV and having a threshold at which the derivative of the voltage (dV/dt) was greater than 10mV/ms. Rheobase was defined as the minimum amount of current injected that resulted in at least 1 AP, using 1 second sweeps with 20pA intervals. AP threshold was calculated from the first AP elicited during the rheobase sweep and was defined as the first point at which the voltage rate of change was greater than 10mV/ms. Input resistance was calculated using the change in steady state current in response to a small hyperpolarizing voltage step. AP amplitude was calculated by subtracting threshold voltage from

peak voltage. The action potential duration (APD) 50 was calculated by subtracting the time of AP threshold from the time of achievement of 50% repolarization. The current/frequency plot was based on the average steady state firing frequency calculated at each current step. The same data were used for the fold-rheobase plot by normalizing the current to each cell's rheobase and using only the integer values of fold-rheobase.

Electroencephalogram Recording

Surgical procedures were performed as previously described.[17] Simultaneous electroencephalogram (EEG) recording and

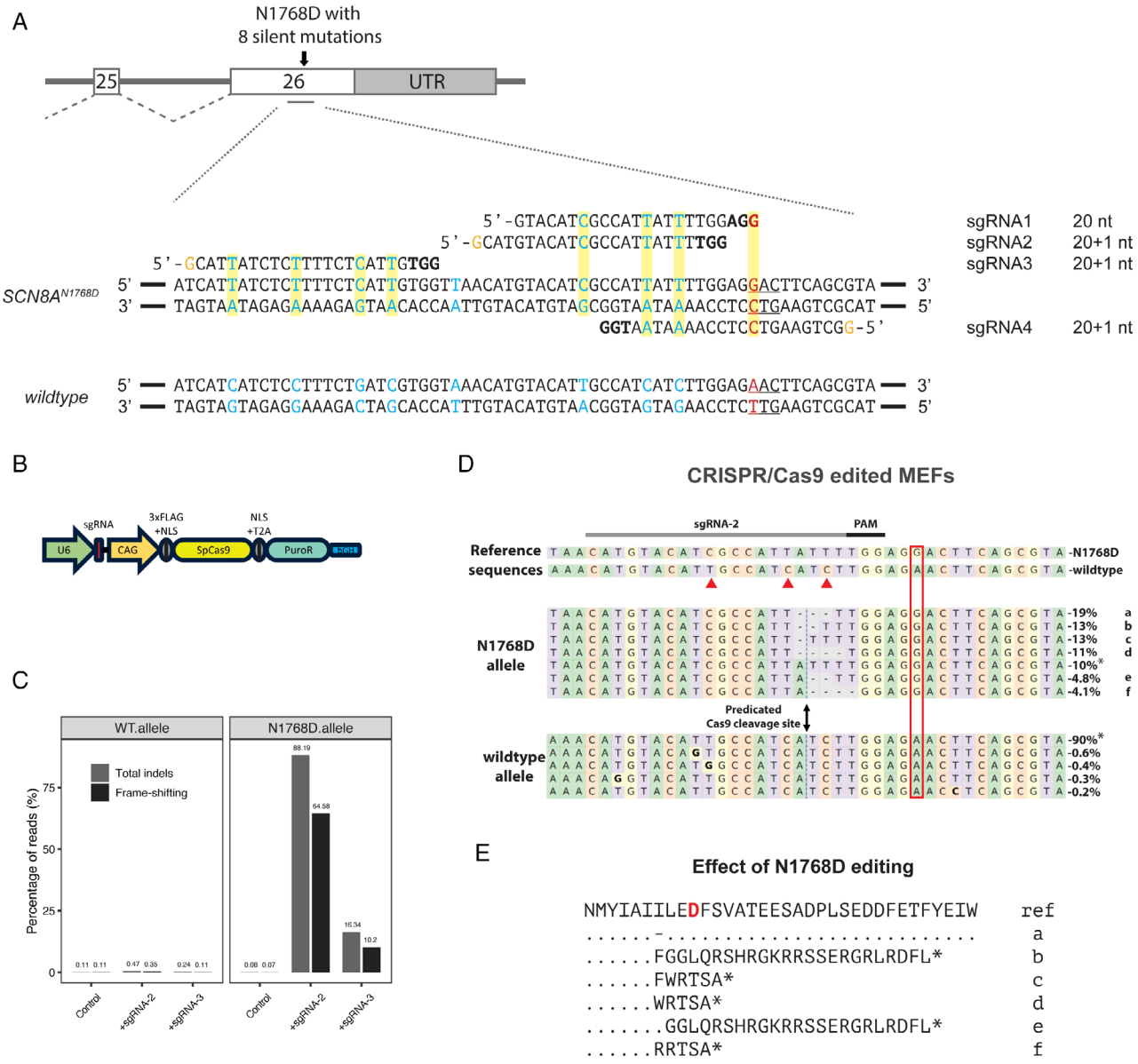

FIGURE 1: Editing of the *Scn8a*^{N1768D} allele in heterozygous *Scn8a*$^{N1768D/+}$ mouse embryonic fibroblasts (MEF) cells. (A) The *Scn8a*^{N1768D} causal mutation is an A to G substitution at residue 1768 (shown in red). The N1768D allele was designed with 8 additional silent base substitutions (blue) within 50 bp of the pathogenic mutation. Four sgRNAs were designed specific for the mutant allele containing 3 or 4 mismatches to the WT allele (yellow). The protospacer adjacent motif (PAM) sequence is shown in bold. (B) PX459 vector insert for sgRNA expression. (C) Allele-specific editing of the *Scn8a*^{N1768D} allele in heterozygous D/+ MEF cells. Editing efficiency of sgRNA-2 and sgRNA-3. The sequencing depth of control, sgRNA-2, and sgRNA3 experiments were 4.6×10^5, 2.6×10^5, and 5.2×10^5, respectively. (D) Graphic representation of indels from MEFs transfected with sgRNA-2 plasmid. Three silent base substitutions in the sgRNA that mark the mutant allele are indicated by red triangles. The A to G substitution causing *Scn8a*-N1768D is in red box. *Sequence identical to the corresponding reference sequences; base substitutions are shown in bold; deletions are represented by dashes. (E) Indels in the mutant allele generated in-frame stop codons and truncation of the C-terminal protein domain, which is known to inactivate the channel.[36] The pathogenic D residue is shown in red. sgRNA = single guide RNA; WT = wild-type.

video monitoring were performed with a Natus recording system continuously for 14 days. Signals were acquired at 1024Hz. Seizures and interictal backgrounds were assessed manually by an experienced reader. Interictal epileptiform discharges and seizures were defined as previously described.[17,35]

Results

Allele-Specific Targeting of the Scn8a^{N1768D} *Allele in Cultured MEFs*

Scn8a$^{N1768D/+}$ mice (designated D/+) carry the *Scn8a* patient variant N1768D, an A to G substitution in the codon for the last residue of the S6 transmembrane

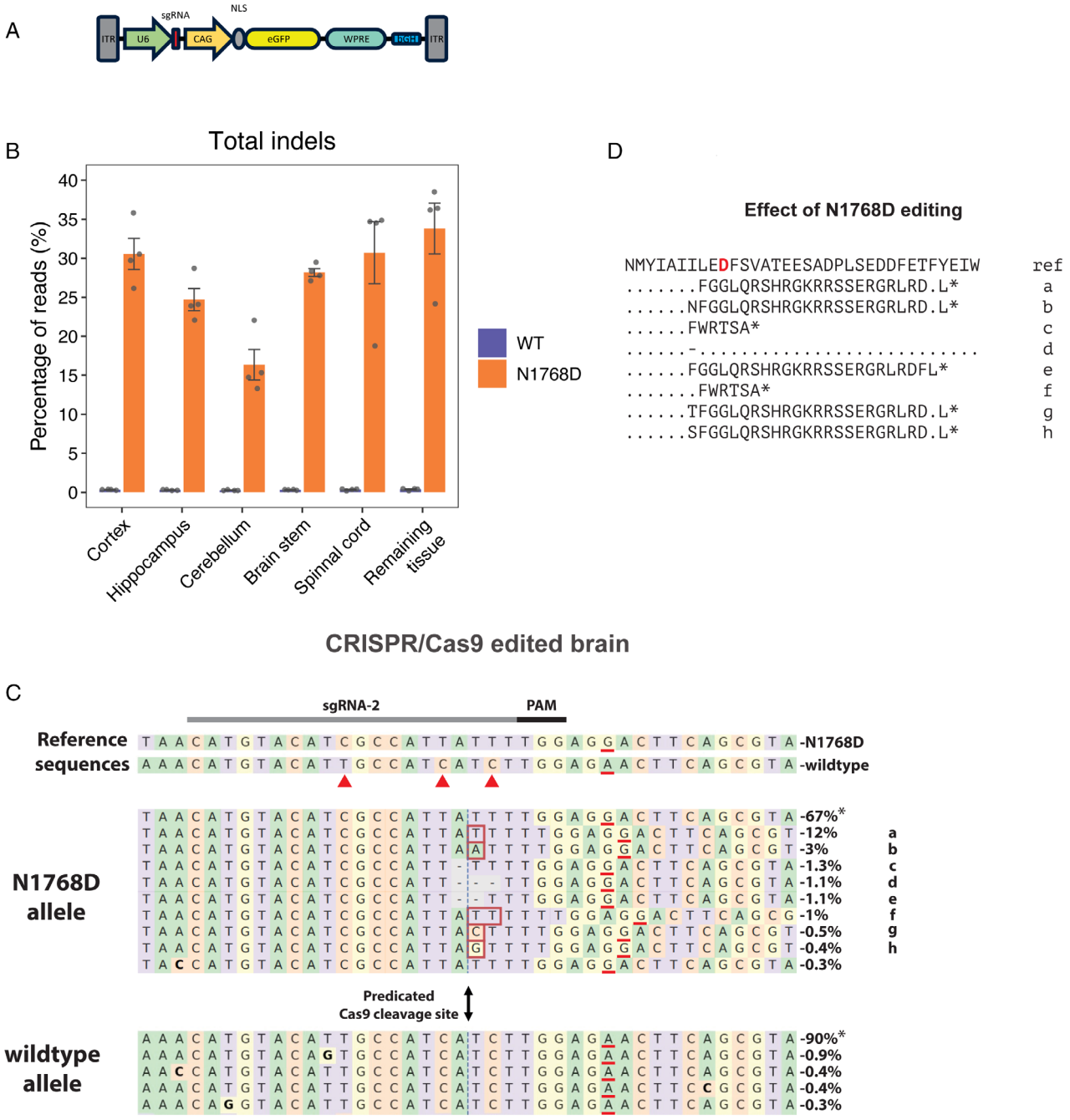

FIGURE 2: Editing of the *Scn8a*^{N1768D} allele in mouse brain. (A) AAV-PHP.eB viral construct for sgRNA-2 expression. (B) Editing efficiency in AAV-PHP.eB treated D/+, Cas9/+ mouse brain (n = 4). The sequencing depth for each experiment group was between 4×10^5 and 16×10^5. (C) Indels from cortex of an AAV-PHP.eB treated D/+, Cas9/+ mouse. The silent base substitutions in the sgRNA that are specific for the mutant allele are marked by red triangles. A to G substitution causing the *Scn8a*-N1768D mutation is underlined. *Sequence identical to the corresponding reference sequences. Bold, substitutions; box, insertions; −, deletions. (D) Indels in the mutant allele resulted in generation of in-frame stop codons and truncation of C-terminal protein sequence. The pathogenic D residue is shown in red. sgRNA = single guide RNA.

TABLE. Editing Efficiency of the *Scn8a*^{N1768D} and Wild-Type Alleles in Heterozygous Brain.

Brain region	1	2	3	4	Mean ± SD
Editing efficiency of the *Scn8a*^{N1768D} allele: % of reads with indels					
Cortex	31	26	30	36	30 ± 4%
Hippocampus	24	22	24	29	25 ± 3%
Cerebellum	15	13	15	22	16 ± 4%
Brain stem	28	27	29	28	28 ± 1%
Spinal cord	35	35	35	19	31 ± 8%
Residual	36	38	36	24	34 ± 6%
Editing efficiency of the wild-type allele: % of reads with indels					
Cortex	0.37	0.34	0.27	0.34	0.33 ± 0.04%
Hippocampus	0.33	0.34	0.24	0.26	0.3 ± 0.05%
Cerebellum	0.24	0.24	0.24	0.33	0.26 ± 0.05%
Brain stem	0.35	0.34	0.31	0.26	0.31 ± 0.04%
Spinal cord	0.42	0.41	0.34	0.19	0.34 ± 0.11%
Residual	0.45	0.45	0.39	0.2	0.37 ± 0.12%

D/+, Cas9/+ mice received ICV injection of AAV-PHP.eB-sgRNA-2 virus at P1. Two months later, RNA was extracted from 6 brain regions and converted to cDNA. The editing efficiency of the *Scn8a*^{N1768D} allele and the wild-type allele were determined by Amplicon-EZ next-generation sequencing. Each column represents 1 animal.
cDNA= complementary DNA; ICV = intracerebroventricular; SD = standard deviation.

segment.[9] Eight silent base substitutions were introduced nearby in the TALEN generation of the mutant mouse (Fig 1A).[29] Four mutant-specific sgRNAs were designed with 3 or 4 mismatches to the WT allele (see Fig 1A). sgRNA-2 and sgRNA-3 exhibited excellent allele-specificity in an in vitro DNA digestion assay (Fig S1) and were selected for subsequent verification in tissue culture.

D/+ MEFs were isolated from E13.5 embryos and maintained in culture. sgRNA-2 and sgRNA-3 were cloned into plasmid PX459 for co-expression of SpCas9 and the puromycin resistance gene (Fig 1B). MEFs were transfected with each plasmid and selected with puromycin, followed by genomic DNA extraction, PCR amplification and targeted next-generation sequencing. In MEFs transfected with sgRNA-2, indels were detected in 88% of the reads that mapped to the mutant allele, but only <0.5% of the reads that mapped to the wild allele, demonstrating strong allele-specificity (see Fig 1). Three quarters of the indels in the mutant allele resulted in frame-shifting, generating a nearby downstream in-frame stop codon with protein truncation in the C-terminal cytoplasmic domain. Loss of this domain is known to result in loss of channel activity.[36]

Transfection with sgRNA-3 plasmid also resulted in allele-specific editing of the mutant allele, but with only 16% efficiency (Fig 1C). sgRNA-2 was selected for in vivo evaluation based on the higher efficiency of pathogenic allele editing in cultured MEFs.

Allele-Specific Editing of the Scn8a^{N1768D} *Variant in Mouse Brain*

sgRNA-2 was packaged into AAV-PHP.eB, which preferentially transduces central nervous system (CNS) neurons with high efficiency (Fig 2).[34] D/+ mice were crossed with Cas9/Cas9 homozygotes carrying a ubiquitously expressed SpCas9 transgene.[37] D/+, Cas9/+ mice, and +/+ Cas9/+ littermate controls were recovered in approximately 1:1 ratio (38:34). At P1, D/+, Cas9/+ mice received 2μl of AAV-PHP.eB-sgRNA-2 (1×10^{13}vg/ml) virus by ICV injection. At 2 months post treatment, cDNA was prepared from brain RNA (n = 4) for targeted next-generation sequencing. Indels at the predicted Cas9 cleavage site were present in the *Scn8a*^{N1768D} allele with 25% to 34% editing efficiency in most brain regions (see Fig 2B,C, Table). Cerebellum

had a lower editing efficiency of 16%. In the WT allele, the frequency of indels was <0.4% (Table). Ninety-two to 94% of indels in the mutant allele resulted in disruption of the reading frame (Fig S2) and premature termination of translation. The edits are located in the final exon of *Scn8a*, and most edited transcripts escaped nonsense-mediated decay (Fig S3).

Allele-Specific Inactivation of the Scn8a^{N1768D} *Allele Protects against Seizures and Lethality*

To assess the effect of genome editing on survival, D/+, Cas9/+ mice were treated on P1 by ICV administration of 2μl virus. Eight of 10 virus-treated mice survived for more than 1 year and are alive at the time of publication (Fig 3A). D/+, Cas9/+ mice of the control cohort

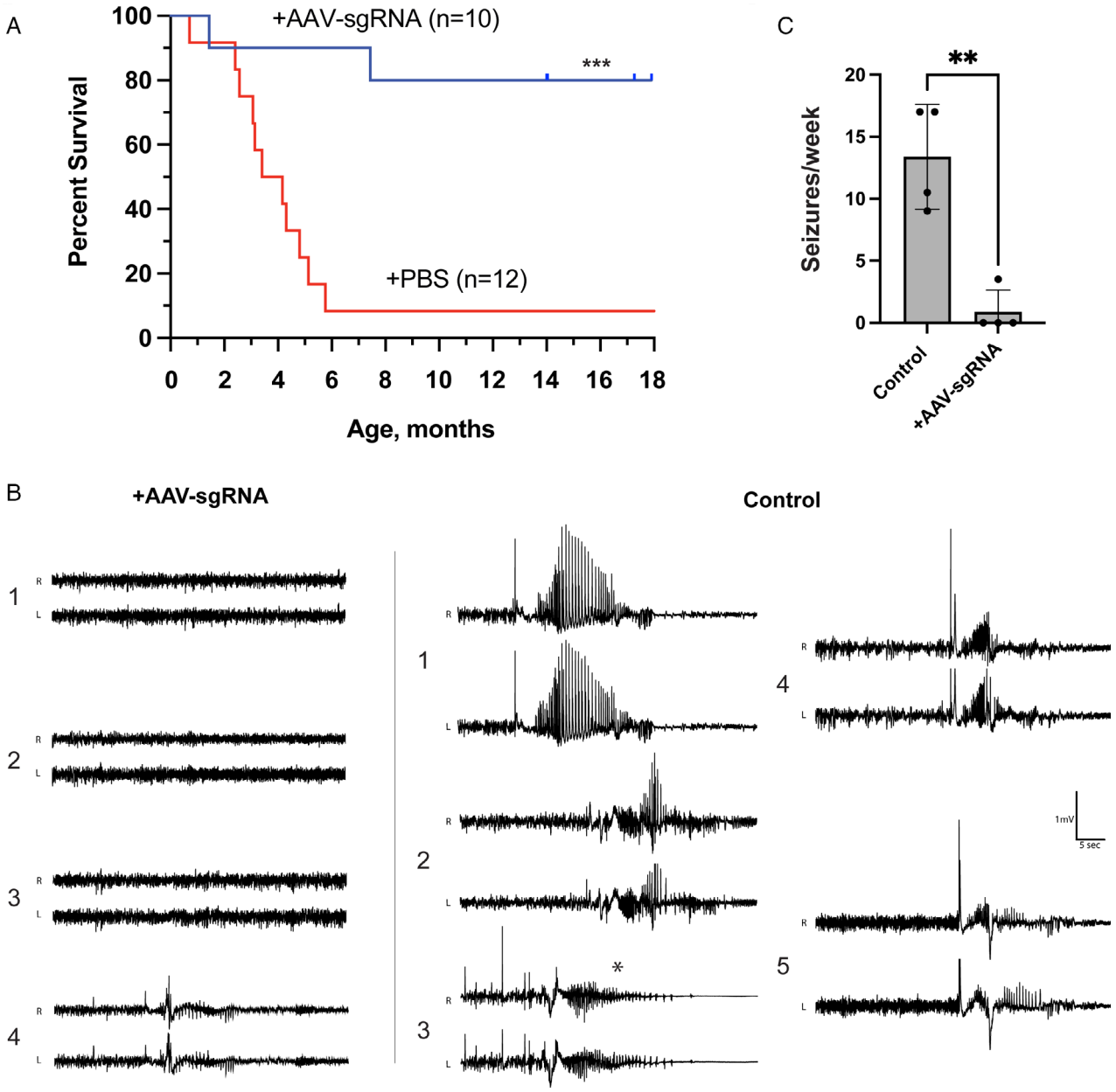

FIGURE 3: Allele-specific inactivation of the *Scn8a*^{N1768D} allele rescues lethality and seizures. (A) Survival. D/+, Cas9/+ mice were treated by intracerebroventricular (ICV) administration on postnatal day 1 (P1) with AAV-PHP.eB-sgRNA-2 or PBS (***$p < 0.001$, log-rank [Mantel-Cox] test). (B) Seizures. Mice were monitored for 2 weeks by continuous video/electroencephalography monitoring. Representative traces from each animal were recorded by right and left epidural electrodes. Left: 3 of 4 D/+, Cas9/+ mice that received AAV treatment were completely protected from electrographic and convulsive seizures; the fourth AAV-treated mouse had occasional seizures. Right: Control D/+, Cas9/+ mice received PBS and exhibited both electrographic and behavioral seizures. *Death during recording. (C) Seizure frequency. (**$p < 0.01$, unpaired *t* test). PBS = phosphate-buffered saline; sgRNA = single guide RNA. [Color figure can be viewed at www.annalsofneurology.org]

received 2µl of PBS by ICV. Median survival of PBS-treated controls was 4 months. Therefore, treatment significantly extended the survival of D/+, Cas9/+ mice ($p < 0.001$, log-rank [Mantel-Cox] test).

To examine the effect of treatment on seizure incidence, 4 AAV-treated D/+, Cas9/+ mice were monitored at 5 to 6 months of age by video/EEG recording for 14 days. Three of 4 mice remained seizure-free during the recording period and the fourth exhibited a low rate of 3.5 seizures/week (Fig 3B,C). In contrast, the 5 PBS-treated D/+, Cas9/+ controls exhibited frequent seizures (see Fig 3B,C), including one that experienced a terminal seizure on day 6. The seizure phenotype in control mice was consistent with previous observations.[18,30] Seizure frequency was significantly reduced by AAV treatment (see Fig 3C). The percent of seizure-free mice increased from 0/5 in PBS-treated mice to 3/4 in the AAV-treated mice ($p < 0.05$, χ^2 test). Targeted inactivation of the pathogenic allele was protective against both seizures and lethality.

Inactivation of the Scn8a^{N1768D} *Allele Reduces Excitability in Dentate Gyrus Granule Cells*

Previous studies identified elevated neuronal activity in several types of neurons from D/+ mice, including hippocampal CA1 and CA3 neurons,[13] dentate gyrus granule cells,[38] and medial entorhinal cortex neurons.[39] We investigated the effect of editing on electrophysiological properties of dentate gyrus granule cells, because their activation can influence seizure susceptibility,[40] and they exhibit differentially expressed genes after chronic seizures.[38] Mice with genotype D/+, Cas9/+ were treated on P1 by ICV

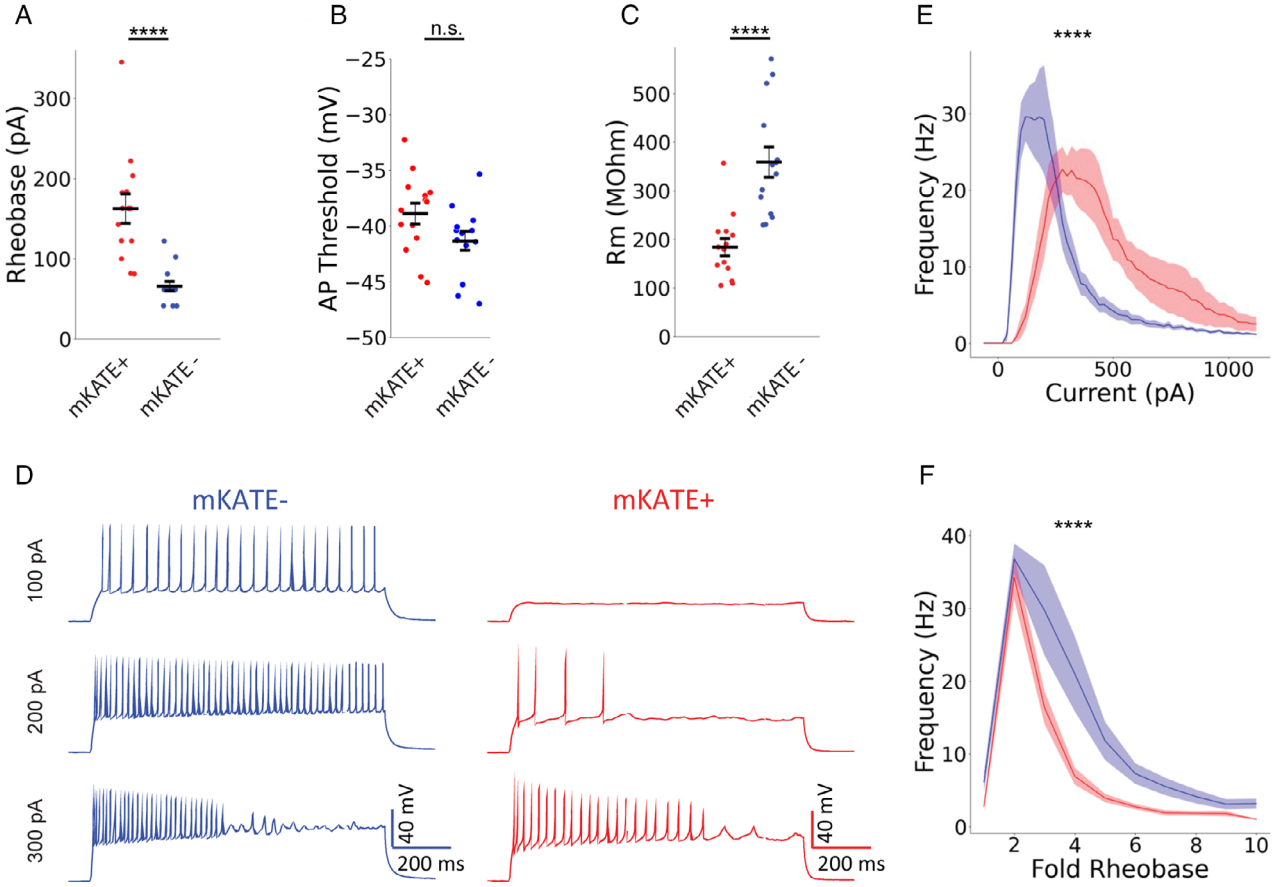

FIGURE 4: Cellular effects of editing: decreased excitability in transduced dentate gyrus granule cells. Mice were injected intracerebroventricularly (ICV) on postnatal day 1 (P1) with the AAV-PHP.eB-sgRNA-2 virus expressing the red fluorescent mKATE marker and recordings were made from transduced (red fluorescent) and non-transduced dentate gyrus granule cells (GCs). (A) The rheobase of transduced (mKATE$^+$) cells (red) (162 ± 18 pA) was significantly higher than that of non-transduced (mKATE$^-$) cells (blue) (66 ± 6 pA). (B) mKATE$^+$ and mKATE$^-$ cells had a similar action potential threshold. (C) The input resistance of transduced mKATE$^+$ GCs was reduced to almost half that of mKATE$^-$ GCs (183 ± 18 vs. 359 ± 31MOhm). (D) Representative current clamp recordings of evoked action potentials elicited by increasing current injections from GCs. (E) The current/frequency (I-f) plot for transduced mKATE$^+$ GCs (red) was right-shifted, reflecting the higher rheobase. (F) I-f plot with current normalized to the rheobase of each class of cells. The curve for transduced mKATE$^+$ cells (red) had a similar rise and faster decay compared with mKATE$^-$ GCs. GCs were recorded from 4 mice; n = 14 mKATE$^+$, n = 14 mKATE$^-$. ****p = <0.0001; unpaired *t* test (A–C) or 2-way ANOVA (E–F). Line and shaded areas represent mean and standard error of the mean.

injection of the AAV.PHP.eB-sgRNA-2 virus carrying the mKATE cassette, which expresses a red fluorescent marker. Acute brain slices were prepared 2 months after treatment. Transduced (mKATE positive) neurons were identified by their red fluorescence and recorded to determine whether viral infection had altered their intrinsic excitability. Nearby non-transduced neurons (mKATE negative) in the same slices were recorded as negative controls. mKATE positive granule cells had a significantly higher rheobase compared to mKATE negative cells, likely because of lower input resistance as opposed to higher action potential threshold (Fig 4A–C). In mKATE positive cells, the amplitude of the first action potential was increased to 81.4 ± 1.2mV compared with 72.2 ± 3.4mV in mKATE negative cells ($p = 0.03$). The APD 50 was reduced to 1.01 ± 0.02ms in the transduced cells compared with 1.07 ± 0.03 seconds ($p = 0.001$) in non-transduced cells. A similar increase in the duration of the action potential was previously seen in hippocampal CA1 neurons of D/+ mice relative to WT.[13] In response to small current injections, mKATE positive granule cells fired fewer action potentials, as seen in example traces (see Fig 4D,E) and in the right-shifted current/frequency (I-f) plot. Normalizing the I-f plot to rheobase (see Fig 4F) eliminated the right-shift, suggesting that this difference was attributable to the higher rheobase of transduced mKATE positive granule cells. (A significant difference persisted in response to larger current injections.) Therefore, intrinsic neuronal excitability was reduced by transduction with the sgRNA-2 virus.

Assessment of Movement in Mice with Reduced Expression of Pathogenic Scn8a^{N1768D} *Allele*

To detect potential deleterious effects of *Scn8a* editing, D/+, Cas9/+, and +/+, Cas9/+ littermates were treated with AAV-PHP.eb-sgRNA-2 on P1 and examined at 6 months of age for behavior in the open field test. The 2 groups did not differ in distance traversed, average velocity, or time at rest in the open field (Fig 5A–C).

In previous studies, the D/+ mice did not exhibit a motor phenotype in the open field test.[30] Reduction of *Scn8a* expression to 50% of WT level by ASO did not cause motor deficits in these mice.[16,18] In this study, the 30% editing in the D/+ mice also failed to impair motor

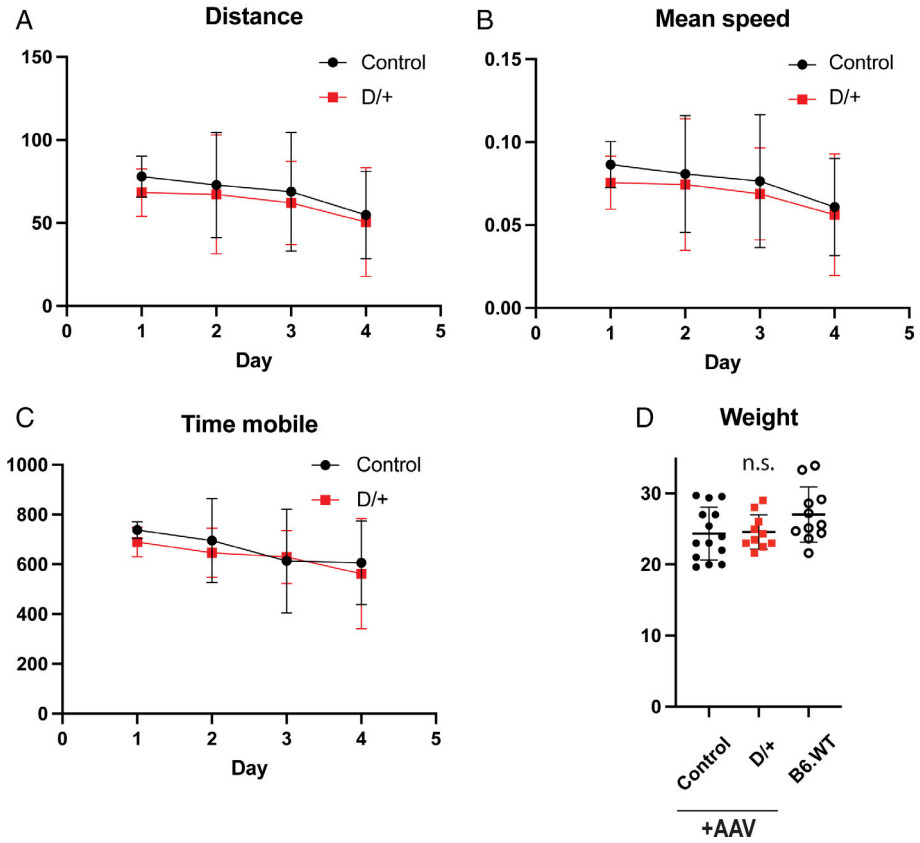

FIGURE 5: Open field test of D/+, Cas9/+ mice after allele-specific editing. D/+, Cas9/+ mice (n = 5) and +/+, Cas9/+ littermates (n = 6) were treated with AAV-PHP.eB-sgRNA-2 virus at postnatal day 1 (P1). At 6 months of age, behavior in the open field test was monitored for 15 minutes on 4 successive days. (A–C) The activity of treated mutant mice did not differ significantly from treated control mice. (D) Absence of deleterious impact of viral treatment is indicated by normal body weight of mice at 6 months of age, compared with untreated wild-type mice. Mean ± standard deviation. [Color figure can be viewed at www.annalsofneurology.org]

function. There were no signs of failure to thrive as a result of the reduced expression of the *Scn8a*^{N1768D} allele, and bodyweight was unaffected at 6 months of age (see Fig 5D). Therefore, AAV-PHP.eB mediated *Scn8a*^{N1768D} allele inactivation was well tolerated.

Discussion

We examined the efficacy of allele-specific editing of the dominant epileptogenic variant *Scn8a*^{N1768D} by CRISPR/Cas9 in brain. Neuronal targeting was achieved using the AAV-PHP.eB virus and allele specificity was based on several mismatches between *Scn8a*^{N1768D} and the WT allele. Viral delivery of an allele-specific sgRNA generated out-of-frame indels predominantly in the mutant allele, achieving 25 to 34% editing efficiency throughout the cerebrum and spinal cord, with lower efficiency (16%) in cerebellum. This effect was sufficient to rescue survival and suppress seizures in the mutant mice, without obvious adverse effects. Our results demonstrate that allele-specific inactivation of pathogenic *Scn8a* alleles is attainable in the brain of a heterozygous variant at a sufficient frequency to rescue seizures and lethality.

Scn8a is broadly expressed in neurons throughout the CNS and peripheral nervous system. Precision medicine for GOF variants of *Scn8a* must achieve a sufficient reduction in expression to ameliorate the major pathology without the detrimental side effects of $Na_v1.6$ deficiency.[41–43] A significant advantage of allele-specific targeting is that the maximum reduction of expression is 50%, preventing the development of more severe adverse effects than those seen with haploinsufficiency.

After ICV administration of the AAV-PHP.eB virus, editing efficiency was high throughout the brain. Previous studies demonstrated the importance of cortex and hippocampus in GOF *Scn8a* epilepsy. For example, expression of the GOF *Scn8a*^{R1872W} in forebrain excitatory neurons was sufficient to induce seizures and sudden death.[12] There is elevated activity in hippocampal CA1, CA3, and granule neurons from *Scn8a*-DEE mice.[12,38] Downregulation of *Scn8a*^{N1768D} expression in the dentate gyrus region of the hippocampus by an *Scn8a*-shRNA extended survival in D/+ mice.[38] Hyperexcitability was also reported in entorhinal cortex neurons from D/+ mice.[39] These studies suggest that inactivation of the *Scn8a*^{N1768D} allele in cortex and hippocampus contributes to the positive outcome. Despite the epileptic phenotype, untreated D/+ mice do not exhibit impaired motor function. In the current work, the cerebellum had somewhat lower editing efficiency of 16% that did not lead to obvious adverse effects on motor function. The cerebellum has limited surface area contacting the fourth ventricle, which likely resulted in less efficient diffusion of virus. The effect of 30% editing in brain stem and remaining tissues remains to be studied.

It is interesting to compare this work with our previous administration of an ASO complementary to the 3′ untranslated region of the *Scn8a* transcript.[16] The ASO rescued survival by reducing the overall abundance of *Scn8a* transcript to 50% of normal, with comparable effect predicted for both alleles. In comparison, allele-specific CRISPR/Cas9 targeting rescued survival with only 25% editing of the mutant transcript, or 12% reduction of functional *Scn8a* transcripts. Therefore, the allele-specific treatment could be considered more efficient.

Inactivation of the *Scn8a*^{N1768D} allele in between 1/4 and 1/3 of neurons was sufficient to prevent seizures and lengthen survival in our studies. How does allele-specific inactivation achieve seizure protection in vivo? CRISPR/Cas9 editing of the pathogenic allele deletes the C-terminal domain of the channel protein and generates a functionally null allele.[36,44] Neurons with inactivation of the pathogenic variant express a single active WT allele. When comparing the intrinsic excitability of AAV-PHP.eB-sgRNA-2 transduced (mKATE positive) and non-transduced (mKATE negative) granule cells, we found that transduced cells had significantly higher rheobase compared to adjacent non-transduced granule cells patched within the same slices. In other words, the amount of current required to depolarize the transduced granule cells to action potential threshold was significantly higher than non-transduced cells. Therefore, the cells with loss of the GOF channel were hypoexcitable compared with the non-transduced neurons. This effect likely contributes to seizure reduction in vivo.

Previous work identified decreased rheobase in neurons expressing pathogenic GOF *Scn8a* variants such as p.(Arg223Gly),[45] p.(R1872W),[11] and p.(N1768D).[14] Further study will be required to elucidate the precise mechanism by which *Scn8a* editing contributes to increased rheobase in granule cells, and the generalizability of our granule cell data to other cell types and brain regions. In a previous study, we reported a significant increase of firing frequency in D/+ dentate gyrus granule cells, with no difference in rheobase or individual properties of the first AP at rheobase.[38] In the current study, knockout of the mutant N1768D allele decreased firing frequency, but also changed rheobase and AP waveforms. The haploinsufficiency of *Scn8a* in edited cells might contribute to these changes. It is also possible that partial reduction of $Na_v1.6$ expression causes elevated expression of $Na_v1.2$ channels, as previously shown in null cortical pyramidal neurons.[46] The mechanism by which reduced

excitability of 25% of neurons disrupts circuit hypersynchrony remains to be determined.

The allele-specific CRISPR-Cas9 (CRISPRi) editing described here used a cluster of 3 base mismatches in the sgRNA between WT and mutant alleles. However, most human pathogenic alleles contain a single nucleotide substitution, which can only be targeted with current CRISPR/Cas9 if the substitution generates a new protospacer adjacent motif (PAM) site or is located very close to the PAM site of the sgRNA. In addition, CRISPRi inactivation of the mutant allele involves a double-stranded break in chromosomal DNA with potential deleterious off-target effects. Clinical application will require different gene-editing technology, such as base editing or prime editing. Base editing has good editing efficiency and allele specificity, but the targeted base must be located in the editing window determined by the matching PAM site. Base editors may also produce undesired bystander edits because all suitable bases within the editing window could be modified potentially generating new mutations. Prime editing avoids bystander editing, but has low editing efficiency. Our demonstration of the efficacy of allele-specific inactivation of 1/4 to 1/3 of a dominant *SCN8A* variant demonstrates "proof of principle" for efforts to develop base editing and prime editing therapies for *SCN8A*-DEE and related disorders.

Despite the introduction of many new antiepileptic drugs in the past 30 years, approximately 1/3 of patients remain drug-resistant. Several hundred different *SCN8A* variants have been described in patients with DEE, varying in functional deficit and causing a spectrum of clinical severity.[3,4,10,11] The level of editing required for a therapeutic response may depend on the functional effect of each variant. Many individuals with *SCN8A*-DEE experience unremitting seizures, sleep and gastric disturbances, and elevated risk of SUDEP.[4,6] Therefore, even partial therapeutic efficacy could be valuable. Recommendations summarizing current treatments have recently been published.[47,48] Genetic therapies that reduce expression of GOF *Scn8a* variants, using ASOs or CRISPRi, prevent seizures and prolong healthy life in mouse models. Translation of these preclinical observations to clinical application is an urgent priority for the future.

Acknowledgements

This work was supported by NINDS (grants R01-NS34509, M.H.M.; K08-NS121464, J.M.; and K08-NS124937, J.Z.) The AAV-PHP.eB viruses expressing *Scn8a* sgRNAs were prepared in the University of Michigan Vector Core (T. Lanigan, Director).

Author Contributions

W.Y., J. M. and M.H.M. contributed to the conception and design of the study. W.Y., S.F.H., Y.H., L.Z., Y.D., J.Z., and F.R. contributed to the acquisition and analysis of data. W.Y., Y.H., X.J., J.M., and M.H.M. contributed to drafting the text and preparing figures.

Potential Conflicts of Interest

Nothing to report.

Data Availability

All relevant data are included in the manuscript.

References

1. Zack MM, Kobau R. National and state estimates of the numbers of adults and children with active epilepsy-United States, 2015. MMWR Morb Mortal Wkly Rep 2017;66:821–825. https://doi.org/10.15585/mmwr.mm6631a1.
2. Guerrini R, Conti V, Mantegazza M, et al. Developmental and epileptic encephalopathies: from genetic heterogeneity to phenotypic continuum. Physiol Rev 2023;103:433–513. https://doi.org/10.1152/physrev.00063.2021.
3. Meisler MH, Helman G, Hammer MF, et al. SCN8A encephalopathy: research progress and prospects. Epilepsia 2016;57:1027–1035. https://doi.org/10.1111/epi.13422.
4. Johannesen KM, Gardella E, Encinas AC, et al. The spectrum of intermediate SCN8A-related epilepsy. Epilepsia 2019;60:830–844. https://doi.org/10.1111/epi.14705.
5. Sanders SJ, Campbell AJ, Cottrell JR, et al. Progress in understanding and treating SCN2A-mediated disorders. Trends Neurosci 2018;41:442–456. https://doi.org/10.1016/j.tins.2018.03.011.
6. Johannesen KM, Liu Y, Koko M, et al. Genotype-phenotype correlations in SCN8A-related disorders reveal prognostic and therapeutic implications. Brain 2022;145:2991–3009. https://doi.org/10.1093/brain/awab321.
7. Hu C, Luo T, Wang Y. Phenotypic and genetic spectrum in Chinese children with SCN8A-related disorders. Seizure 2022;95:38–49. https://doi.org/10.1016/j.seizure.2021.12.011.
8. Meisler MH, Hill SF, Yu W. Sodium channelopathies in neurodevelopmental disorders. Nat Rev Neurosci 2021;22:152–166. https://doi.org/10.1038/s41583-020-00418-4.
9. Veeramah KR, O'Brien JE, Meisler MH, et al. De novo pathogenic SCN8A mutation identified by whole-genome sequencing of a family quartet affected by infantile epileptic encephalopathy and SUDEP. Am J Hum Genet 2012;90:502–510. https://doi.org/10.1016/j.ajhg.2012.01.006.
10. Vanoye CG, Abramova TV, DeKeyser JM, et al. Molecular and cellular context influences SCN8A variant function. JCI Insight 2024;9:e177530. https://doi.org/10.1101/2023.11.11.566702.
11. Liu Y, Schubert J, Sonnenberg L, et al. Neuronal mechanisms of mutations in SCN8A causing epilepsy or intellectual disability. Brain 2019;142:376–390. https://doi.org/10.1093/brain/awy326.
12. Bunton-Stasyshyn RKA, Wagnon JL, Wengert ER, et al. Prominent role of forebrain excitatory neurons in SCN8A encephalopathy. Brain 2019;142:362–375. https://doi.org/10.1093/brain/awy324.
13. Lopez-Santiago LF, Yuan Y, Wagnon JL, et al. Neuronal hyperexcitability in a mouse model of SCN8A epileptic encephalopathy. Proc Natl Acad Sci U S A 2017;114:2383–2388. https://doi.org/10.1073/pnas.1616821114.

14. Wengert ER, Miralles RM, Wedgwood KCA, et al. Somatostatin-positive interneurons contribute to seizures in SCN8A epileptic encephalopathy. J Neurosci 2021;41:9257–9273. https://doi.org/10.1523/JNEUROSCI.0718-21.2021.

15. Miralles RM, Boscia AR, Kittur S, et al. Parvalbumin interneuron impairment leads to synaptic transmission deficits and seizures in SCN8A epileptic encephalopathy. bioRxiv 2024. https://doi.org/10.1101/2024.02.09.579511.

16. Lenk GM, Jafar-Nejad P, Hill SF, et al. Scn8a antisense oligonucleotide is protective in mouse models of SCN8A encephalopathy and Dravet syndrome. Ann Neurol 2020;87:339–346. https://doi.org/10.1002/ana.25676.

17. Hill SF, Ziobro JM, Jafar-Nejad P, et al. Genetic interaction between Scn8a and potassium channel genes Kcna1 and Kcnq2. Epilepsia 2022;63:e125–e131. https://doi.org/10.1111/epi.17374.

18. Hill SF, Yu W, Ziobro J, et al. Long-term downregulation of the sodium channel gene Scn8a is therapeutic in mouse models of SCN8A epilepsy. Ann Neurol 2023;95:754–759. https://doi.org/10.1002/ana.26861.

19. Wagnon JL, Barker BS, Ottolini M, et al. Loss-of-function variants of SCN8A in intellectual disability without seizures. Neurol Genet 2017;3:e170. https://doi.org/10.1212/NXG.0000000000000170.

20. Wengert ER, Tronhjem CE, Wagnon JL, et al. Biallelic inherited SCN8A variants, a rare cause of SCN8A-related developmental and epileptic encephalopathy. Epilepsia 2019;60:2277–2285. https://doi.org/10.1111/epi.16371.

21. Blanchard MG, Willemsen MH, Walker JB, et al. De novo gain-of-function and loss-of-function mutations of SCN8A in patients with intellectual disabilities and epilepsy. J Med Genet 2015;52:330–337. https://doi.org/10.1136/jmedgenet-2014-102813.

22. Trudeau MM, Dalton JC, Day JW, et al. Heterozygosity for a protein truncation mutation of sodium channel SCN8A in a patient with cerebellar atrophy, ataxia, and mental retardation. J Med Genet 2006;43:527–530. https://doi.org/10.1136/jmg.2005.035667.

23. Lyu H, Bosselmann CM, Johannesen KM, et al. Clinical and electrophysiological features of SCN8A variants causing episodic or chronic ataxia. EBioMedicine 2023;98:104855. https://doi.org/10.1016/j.ebiom.2023.104855.

24. Kearney JA, Buchner DA, De Haan G, et al. Molecular and pathological effects of a modifier gene on deficiency of the sodium channel Scn8a (Na(v)1.6). Hum Mol Genet 2002;11:2765–2775. https://doi.org/10.1093/hmg/11.22.2765.

25. Gyorgy B, Nist-Lund C, Pan B, et al. Allele-specific gene editing prevents deafness in a model of dominant progressive hearing loss. Nat Med 2019;25:1123–1130. https://doi.org/10.1038/s41591-019-0500-9.

26. Gao X, Tao Y, Lamas V, et al. Treatment of autosomal dominant hearing loss by in vivo delivery of genome editing agents. Nature 2018;553:217–221. https://doi.org/10.1038/nature25164.

27. Tao Y, Lamas V, Du W, et al. Treatment of monogenic and digenic dominant genetic hearing loss by CRISPR-Cas9 ribonucleoprotein delivery in vivo. Nat Commun 2023;14:4928. https://doi.org/10.1038/s41467-023-40476-7.

28. Liu X, Qiao J, Jia R, et al. Allele-specific gene-editing approach for vision loss restoration in RHO-associated retinitis pigmentosa. Elife 2023;12. https://doi.org/10.7554/eLife.84065.

29. Jones JM, Meisler MH. Modeling human epilepsy by TALEN targeting of mouse sodium channel Scn8a. Genesis 2014;52:141–148. https://doi.org/10.1002/dvg.22731.

30. Wagnon JL, Korn MJ, Parent R, et al. Convulsive seizures and SUDEP in a mouse model of SCN8A epileptic encephalopathy. Hum Mol Genet 2015;24:506–515. https://doi.org/10.1093/hmg/ddu470.

31. Li H. Aligning sequence reads, clone sequences and assembly contigs with BWA-MEM. arXiv 2013. https://doi.org/10.48550/arXiv.1303.3997.

32. Danecek P, Bonfield JK, Liddle J, et al. Twelve years of SAMtools and BCFtools. Gigascience 2021;10. https://doi.org/10.1093/gigascience/giab008.

33. Clement K, Rees H, Canver MC, et al. CRISPResso2 provides accurate and rapid genome editing sequence analysis. Nat Biotechnol 2019;37:224–226. https://doi.org/10.1038/s41587-019-0032-3.

34. Hana S, Peterson M, McLaughlin H, et al. Highly efficient neuronal gene knockout in vivo by CRISPR-Cas9 via neonatal intracerebroventricular injection of AAV in mice. Gene Ther 2021;28:646–658. https://doi.org/10.1038/s41434-021-00224-2.

35. Kao HY, Hu S, Mihaylova T, et al. Defining the latent period of epileptogenesis and epileptogenic zone in a focal cortical dysplasia type II (FCDII) rat model. Epilepsia 2021;62:1268–1279. https://doi.org/10.1111/epi.16868.

36. Mantegazza M, Yu FH, Catterall WA, Scheuer T. Role of the C-terminal domain in inactivation of brain and cardiac sodium channels. Proc Natl Acad Sci U S A 2001;98:15348–15353. https://doi.org/10.1073/pnas.211563298.

37. Platt RJ, Chen S, Zhou Y, et al. CRISPR-Cas9 knockin mice for genome editing and cancer modeling. Cell 2014;159:440–455. https://doi.org/10.1016/j.cell.2014.09.014.

38. Yu W, Hill SF, Zhu L, et al. Dentate gyrus granule cells are a locus of pathology in *Scn8a* developmental encephalopathy. Neurobiol Disease 2024;199:106591. https://doi.org/10.1016/j.nbd.2024.106591

39. Ottolini M, Barker BS, Gaykema RP, et al. Aberrant sodium channel currents and hyperexcitability of medial entorhinal cortex neurons in a mouse model of SCN8A encephalopathy. J Neurosci 2017;37:7643–7655. https://doi.org/10.1523/JNEUROSCI.2709-16.2017.

40. Mattis J, Somarowthu A, Goff KM, et al. Corticohippocampal circuit dysfunction in a mouse model of Dravet syndrome. Elife 2022;11:69293. https://doi.org/10.7554/eLife.69293.

41. Burgess DL, Kohrman DC, Galt J, et al. Mutation of a new sodium channel gene, Scn8a, in the mouse mutant 'motor endplate disease'. Nat Genet 1995;10:461–465. https://doi.org/10.1038/ng0895-461.

42. Levin SI, Meisler MH. Floxed allele for conditional inactivation of the voltage-gated sodium channel Scn8a (NaV1.6). Genesis 2004;39:234–239. https://doi.org/10.1002/gene.20050.

43. Meisler MH, Kearney J, Escayg A, et al. Sodium channels and neurological disease: insights from Scn8a mutations in the mouse. Neuroscientist 2001;7:136–145. https://doi.org/10.1177/107385840100700208.

44. Jones JM, Dionne L, Dell'Orco J, et al. Single amino acid deletion in transmembrane segment D4S6 of sodium channel Scn8a (Nav1.6) in a mouse mutant with a chronic movement disorder. Neurobiol Dis 2016;89:36–45. https://doi.org/10.1016/j.nbd.2016.01.018.

45. Liu Y, Koko M, Lerche H. A SCN8A variant associated with severe early onset epilepsy and developmental delay: loss- or gain-of-function? Epilepsy Res 2021;178:106824. https://doi.org/10.1016/j.eplepsyres.2021.106824.

46. Katz E, Stoler O, Scheller A, et al. Role of sodium channel subtype in action potential generation by neocortical pyramidal neurons. Proc Natl Acad Sci U S A 2018;115:E7184–E7192. https://doi.org/10.1073/pnas.1720493115.

47. Conecker G, Xia MY, Hecker J, Achkar C, et al. Global modified Delphi consensus on diagnosis, phenotypes, and treatment of SCN8A-related epilepsy and/or neurodevelopmental disorders. Epilepsia, 2024;65:2322–2338. https://doi.org/10.1111/epi.17992

48. Conecker G, Xia MY, Hecker J, Achkar C, et al. Global modified-Delphi consensus on comorbidities and prognosis of SCN8A-related epilepsy and/or neurodevelopmental disorders. Epilepsia, 2024;65:2308–2321. https://doi.org/10.1111/epi.17991